

Iron-porphyrin encapsulated in poly(methacrylic acid) and mesoporous Al-MCM-41 as catalysts in the oxidation of benzene to phenol

Hadi Nur*, Helda Hamid, Salasiah Endud, Halimaton Hamdan, Zainab Ramli

Ibnu Sina Institute for Fundamental Science Studies, Universiti Teknologi Malaysia, 81310 UTM Skudai, Johor, Malaysia

Received 15 March 2005; received in revised form 25 June 2005; accepted 19 July 2005

Abstract

Poly(methacrylic acid) (PMAA) and mesoporous molecular sieve Al-MCM-41 with Si/Al = 20 were used as supports for the encapsulation of bulky iron(III)-5,10,15,20-tetra-(4-pyridyl)porphyrin (Fe-TPyP). Metalloporphyrin of Fe(III) was encapsulated inside the mesopores of Al-MCM-41 by a process of sequential synthesis of Fe-TPyP by treatment of FeCl₃ with 5,10,15,20-tetra-(4-pyridyl) porphyrin (TPyP), followed by encapsulation of Fe-TPyP. Fe-TPyP complexes were also successfully encapsulated in PMAA by polymerizing a monomer (MAA) with a cross-linker around the Fe-TPyP complexes. The materials obtained were identified using XRD, UV-vis DR, FTIR and luminescence spectroscopies. The oxidation of benzene to phenol using aqueous hydrogen peroxide has been studied using both iron-porphyrin encapsulated in poly(methacrylic acid) and mesoporous Al-MCM-41 as catalysts. The encapsulated iron-porphyrin in PMAA (Fe-TPyP-PMAA) give a higher catalytic activity compared to Fe-TPyP encapsulated in Al-MCM-41 (Fe-TPyP-MCM-41). However, the product selectivity and the regenerability of Fe-TPyP-PMAA are not as good as those of Fe-TPyP-MCM-41. One considers that the hydrophobic nature of Fe-TPyP-PMAA may account for the high catalytic activity, and the ordered structure of Fe-TPyP-MCM-41 may contribute to a high selectivity. © 2005 Elsevier B.V. All rights reserved.

Keywords: Encapsulation; Iron-porphyrin; Al-MCM-41; Poly(methacrylic acid); Phenol

1. Introduction

Iron-porphyrin has been the subject of intensive study [1,2] largely because of their ability to catalyze a wide variety of oxidation transformations, e.g. alkenes epoxidation, alkanes hydroxylation, etc. with molecular oxygen. In the last two decades, therefore, increasing attention in catalytic oxidation has been focused on the use of biomimetic systems based on Fe(II), Ru(II) and Mn(II) porphyrin [3–5]. Fig. 1 shows a unique iron-porphyrin structure.

Synthetic metalloporphyrins are widely used as homogeneous catalysts for hydrocarbon oxidation [6–8]. There are, however, several disadvantages in using metalloporphyrins as catalysts in homogeneous oxidation processes. The difficulty in separating the catalysts from the product substantially increases the cost of using homogeneous catalysis in commercial processes. One approach to achieve this goal is to

immobilize homogeneous catalysts on porous solid supports, which simultaneously has the advantages of turning the liquid phase oxidation from homogeneous into heterogeneous. Supporting metalloporphyrins on porous solid supports also provides a physical separation of active sites, thus minimizing catalyst self-destruction and dimerization of unhindered metalloporphyrins [9].

Mesoporous MCM-41 with its hexagonally ordered structure has attracted much attention because of their potential use as catalyst supports [10–14]. Transition metal complexes and organometallic compounds can be encapsulated in the mesoporous MCM-41 supports by physical adsorption or covalent linkage. More recently, much effort was focused on the encapsulation of metalloporphyrins in the pore of MCM-41 [15–18]. For example, Che and coworkers [18] have immobilized a ruthenium porphyrin on modified MCM-41. However, the MCM-41, an inorganic material, is hydrophilic and rigid. In this study, we also propose a procedure to encapsulate iron-porphyrin on the polymer support, namely poly(methacrylic acid) (PMAA). One expects that

* Corresponding author. Tel.: +60 7 5536061; fax: +60 7 5536080.
E-mail address: hadi@kimia.fs.utm.my (H. Nur).

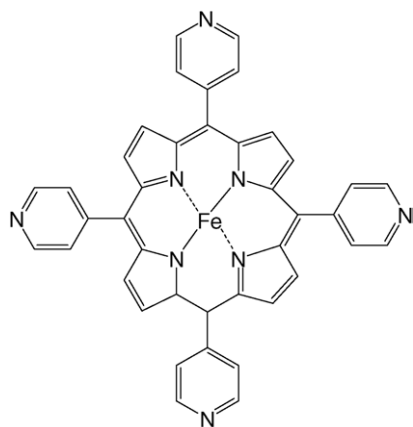


Fig. 1. Iron(III)-tetra-(4-pyridyl)-porphyrin (TPyP).

the flexibility and hydrophobicity of the polymer as support give the advantages in oxidation of organic compounds. Here, we demonstrated the single step liquid phase oxidation of benzene to phenol with aqueous hydrogen peroxide over iron-porphyrin encapsulated in poly(methacrylic acid) in comparison to iron-porphyrin encapsulated in mesoporous Al-MCM-41.

Phenol is produced globally on a scale of £17 billion/year and is expected to maintain an annual growth rate of 4% through the year 2002 due to demand for bisphenol A (polycarbonate resins), phenolic resins and caprolactam (nylon 6) [19]. Phenol is currently produced industrially via the three-step cumene process. Unfortunately, this process is energy intensive, generates considerable waste, and leads to a 1:1 mixture of phenol and acetone [19]. An attractive alternative is the direct oxidation of benzene to phenol using aqueous hydrogen peroxide and a suitable catalyst. A one step process such as this would require less energy and generate zero waste, while producing only phenol.

Selective oxidation of hydrocarbons under mild conditions is of academic interest and industrial importance. In recent years, as a result of increasing environmental constraints, “clean” oxidants such as dioxygen (or air), hydrogen peroxide and alkyl hydroperoxides, which are inexpensive, is becoming more important both in industry and academia, and chemical processes based on cleaner technologies are expected to increase significantly in the next few years.

To the best of our knowledge, there is no report in open literature of the use of iron-porphyrin encapsulated in PMAA in the catalytic oxidation of benzene to phenol with aqueous hydrogen peroxide.

2. Experimental

2.1. Materials and characterizations

Unless otherwise stated, all reagents were of commercial reagent grade and used without further purification.

5,10,15,20-Tetra (4-pyridyl) porphyrin (TPyP) was purchased from Fluka (97%). FeCl₃ anhydrous was purchased from Merck. Methacrylic acid (MAA), ethylene glycol dimethacrylate (EGDMA), α,α' -azoisobutyronitrile (AIBN) were purchased from Fluka.

The samples were characterized by X-ray diffraction (XRD) analysis using Bruker D8 Advance diffractometer with a scanning range of 2θ scale of $1.5\text{--}10^\circ$ using Cu K α radiation ($\lambda = 1.5418 \text{ \AA}$, kV = 40, mA = 40) as the source of radiation.

Infrared spectra were recorded on Shimadzu Fourier transformed infrared (FTIR) 8300 spectrometer. The technique of KBr wafer was used by mixing about 0.25 mg sample with 300 mg KBr powder and then pressed under vacuum ca. 10 tonnes. The pellet was then put in a sample holder to determine its characteristic peaks. IR spectra were set and detected in transmittance (%) rather than absorbance unit. Twenty scans over the range $4000\text{--}400 \text{ cm}^{-1}$ were carried out for all of the sample.

Ultraviolet visible diffuse reflectance (UV–vis DR) spectra were recorded on Lambda 900 spectrometer. Luminescence spectra were recorded on Perkin-Elmer LS 55 spectrometer. About 0.04 g of the sample was placed on a sample holder. After locating and locking sample holder in a proper place in the analyzer, samples were measured in the emission λ (wavelength) scale of $200\text{--}900 \text{ nm}$ at excitation $\lambda = 333 \text{ nm}$.

2.2. Synthesis of Al-MCM-41

The Al-MCM-41 with Si/Al = 20 was synthesized according to Ref. [20]. First, a clear solution of sodium silicate was prepared by combining 2.595 g of 1.00 M aqueous NaOH solution (pellet from Merck) with 10.015 g rice husk ash (90 wt% SiO₂) and the resulting solution (mixture A) was then heated under stirring for 2 h at 80 °C. A mixture of 1.05 g of 25 wt% aqueous NH₃ solution (Merck), 9.115 g of cetyl *N,N,N*-trimethyl ammonium bromide (CTABr) (Fluka) and 1.417 g of NaAlO₂ (54 wt% Al₂O₃, Riedel-de Haen®) were put in a polypropylene bottle and the mixture (mixture B) was then heated with stirring for 1 h at 80 °C. Subsequently, mixture B was added dropwise to a polypropylene bottle containing mixture A with vigorous stirring at room temperature. After stirring for 1 h at 90 °C, the gel mixture in the bottle was heated to 97 °C for 24 h. The CTAluminosilicate gel was then cooled to room temperature. The pH of the reaction mixture was then adjusted to 10.2 by adding 25 wt% acetic acid (CH₃COOH) (Merck). Repeated pH adjustments were performed in order to increase thermal stability and textural uniformity of the product. The heating and pH adjustment procedures were repeated two times. The precipitated product, as-synthesized Al-MCM-41 containing CTA-template was filtered, washed thoroughly with doubly-distilled water and dried in an oven at 97 °C. Al-MCM-41 was calcined in air under static conditions in a muffled furnace. The calcination temperature was increased

from room temperature to 550 °C for 10 h and maintained at 550 °C for 6 h.

2.3. Synthesis of iron-porphyrin (Fe-TPyP)

Iron insertion into TPyP by heating (at 100 °C) TPyP (250 mg, 0.404 mmol) and FeCl₃ anhydrous (100 mg, 0.606 mmol) at reflux in ethanol (30 ml) using oil bath for 1 h. The hot solution was filtered, washed with water and dried under vacuum.

2.4. Synthesis of Fe-TPyP encapsulated in Al-MCM-41 (Fe-TPyP–Al-MCM-41)

Fe-TPyP–Al-MCM-41 was synthesized via the method of Li et al. [9]. A suspension of Al-MCM-41 (250 mg) in methanol containing Fe-TPyP (0.24 mmol) was stirred for 24 h at 20 °C. The resulting materials was filtered and washed with CH₂Cl₂ and acetonitrile until the filtrate becomes colorless. The solid obtained was dried at 100 °C for 4 h which afforded Fe-TPyP.

2.5. Synthesis of iron-porphyrin encapsulated in poly(methacrylic acid) (Fe-TPyP–PMAA)

Fe-TPyP (1 mmol), toluene (12 ml) and MAA (4 mmol) were placed into a 25 ml glass tube and the mixture was left in contact for 10 min. Subsequently, EGDMA (20 mmol) and AIBN (30 mg) were added. The glass tube was sealed and thermostated at 60 °C in an oil bath to start the polymerization process. After 24 h, the obtained micro-spheres were air dried and weighted.

2.6. Catalytic test

Oxidation of benzene was carried out using the above catalysts. Benzene (2 ml), 30% aqueous H₂O₂ (1 ml), catalyst (50 mg) and methanol (2 ml) were placed in a glass tube and the reaction was performed with stirring at 70 °C in an oil bath. GC (Hewlett-Packard 5890 GC Series II) was used to identify the reaction product equipped with a flame ionization detector (FID) and a non-polar capillary column (carbowax). 100 μl of yields was added with 100 μl of internal standard (2-propanol in methanol). Operating conditions of GC were as follows: oven temperature, 50 °C; initial temperature, 50 °C; initial time, 5 min; rate, 10 °C min⁻¹; final temperature, 200 °C; hold time, 5 min. GC/MS (Agilent 6890N-5973 Network Mass Selective Detector) equipped with HP-5MS column (30 m × 0.251 mm × 0.25 μm) was used in order to provide some definite information about the compounds. Sample was analyzed on splitless method with helium (He) as the carrier gas. The samples (0.2 μl) were injected to GC/MS using 10 μl syringes at initial temperature 60 °C without hold time, with rate 15 °C min⁻¹ until 250 °C and hold 2 min.

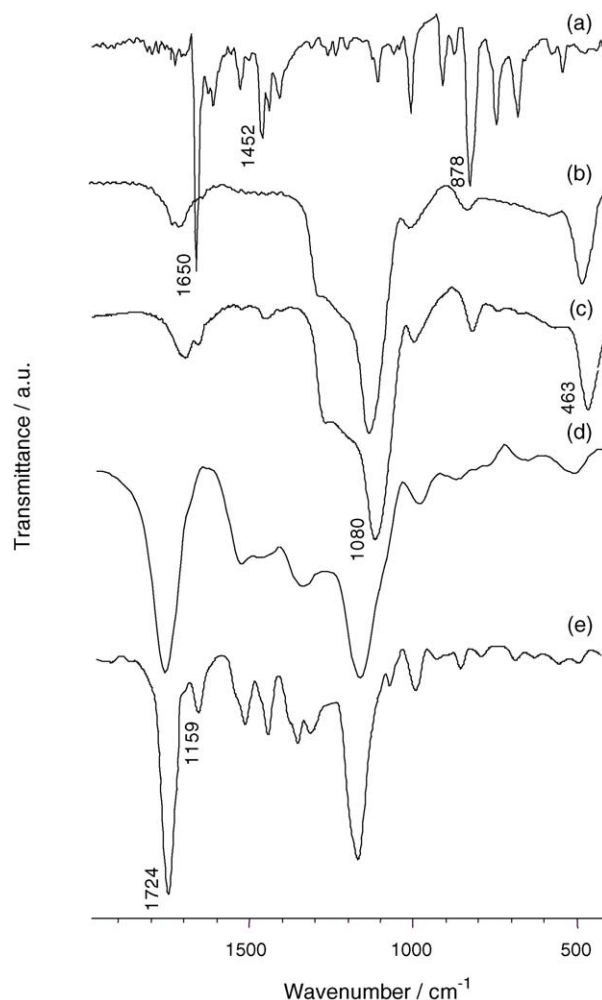


Fig. 2. FTIR spectra of (a) Fe-TPyP, (b) Al-MCM-41, (c) Fe-TPyP–Al-MCM-41, (d) poly(methacrylic acid) (PMAA) and (e) Fe-TPyP–PMAA.

3. Results and discussion

3.1. Characterization of catalysts

The FTIR spectra of Fe-TPyP, Al-MCM-41, Fe-TPyP–Al-MCM-41, poly(methacrylic acid) and Fe-TPyP–PMAA are shown in Fig. 2. The FTIR spectra of Fe-TPyP–Al-MCM-41 and Fe-TPyP–PMAA are in excellent agreement with that of neat Fe-TPyP with additional peaks due to Al-MCM-41 and PMAA, respectively (Fig. 2). The spectrum of Fe-TPyP–PMAA exhibits absorptions at 1724 cm⁻¹ (C=O) and 1159 cm⁻¹ (C–H) which are typical of PMAA, whereas absorptions at around 1100 cm⁻¹ of Fe-TPyP–Al-MCM-41 is typical of Al-MCM-41. Similarly, absorptions at 1650 cm⁻¹ (C=N) and 1452 cm⁻¹ (C–C) are identical with that of free Fe-TPyP. The presence of Fe-TPyP is obvious, because its bands in the region 1700–1300 cm⁻¹ are not observed in the spectrum of the pure Al-MCM-41 and PMAA. This suggests that Fe-TPyPs are structurally unchanged and uniformly distributed in the PMAA and

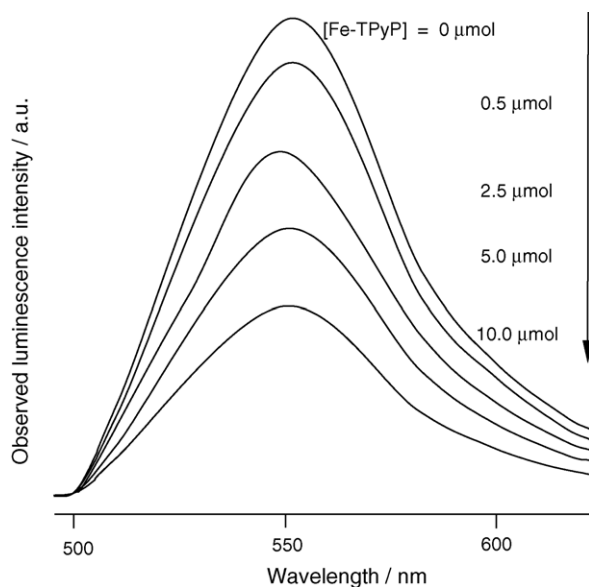


Fig. 3. Luminescence spectrum change of PMAA with various Fe-TPyP concentrations (mole of Fe-TPyP per 1 g of PMAA). The concentration Fe-TPyP was calculated with assuming that the molar amount of Fe is similar to TPyP. The concentration of Fe was analyzed by Atomic Absorption Spectrometer. The excitation wavelength is 333 nm.

Al-MCM-41 matrixes, which proves that Fe-TPyPs preserve their identity after immobilization. Uniform dark-purple powders were obtained in all cases indicating that iron(III) has been included in porphyrin. The IR bands of metal-complexes are weaker due to their low concentration in the PMAA and Al-MCM-41.

Fig. 3 shows the luminescence emission spectrum of Fe-TPyP-PMAA with different amount of Fe-TPyP loading. The quenching behavior of the luminescence was monitored in order to investigate what happened to the luminescence of PMAA after Fe-TPyP loading. It is clear that luminescence intensity of Fe-TPyP-PMAA at around 550 nm decreased with increase of the amount of Fe-TPyP loading. Based on the above results, it is suggested that the Fe-TPyP molecules are encapsulated in high-affinity binding to PMAA.

The Fe-TPyP encapsulated in molecular sieve Al-MCM-41 and PMAA have also been characterized by UV-vis DR spectroscopy and the typical UV-vis DR spectra are given in Fig. 4. In the UV-vis absorption spectrum, the highly conjugated porphyrin macrocycle shows intense absorption at around 400 nm (the Soret band), followed by several weaker absorptions (Q bands) at higher wavelengths (350–600 nm) [21]. Fe-TPyP presents a broad single band at 418 nm and three typical bands attributed to high spin Fe(III)-porphyrin species in the region of 500–700 nm (bands at 516, 557 and 648 nm). The presence of the band at 589 nm in the spectra of Fe-TPyP-Al-MCM-41 (Fig. 4(a)) suggests the occurrence of axial electrostatic interactions between the iron-porphyrin and the anionic Al-MCM-41 pore surfaces [22]. However, these spectra are typical for solutions, and not for the solid-state. Taking into consideration that the interaction between

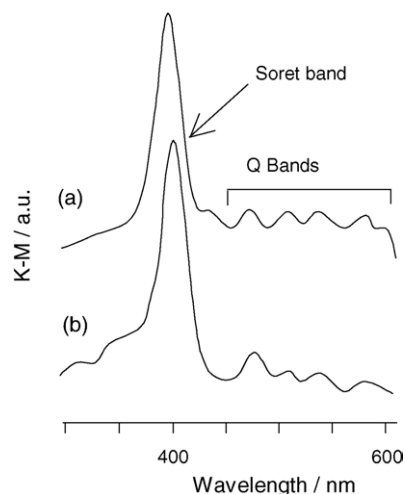


Fig. 4. UV-vis DR spectra of (a) Fe-TPyP-Al-MCM-41 and (b) Fe-TPyP-PMAA.

porphyrin is the dominant interaction in solid-state form, the encapsulation of porphyrin by MCM-41 and PMAA may cause lowering the interaction because porphyrin is now surrounded by MCM-41 and PMMA. This might be the reason why the spectra of Fe-TPyP-Al-MCM-41 and Fe-TPyP-PMAA are almost similar to that of the spectrum of Fe-TPyP in solution.

Since the external surface area of MCM-41 amounts to approximately only $10 \text{ m}^2 \text{ g}^{-1}$ [23], which is related to less than 1% of total surface area, well-dispersed Fe-TPyP can only to a very small extent be situated at the external surface and therefore has to be incorporated inside the mesopores. Theoretically, the surface area of MCM-41 is sufficiently large to accommodate a well-dispersed layer of Fe-TPyP, even at loadings as high as 20 wt% Fe-TPyP in which the expected decrease of surface area of MCM-41 upon Fe-TPyP incorporation is ca. 99%. In view of the fact that calculated amount of Fe-TPyP is only ca. 1%, one should expect that only a small decrease in surface area of MCM-41 could be observed. As tabulated in Table 1 (entries 3 and 5), there was a decrease of ca. 50% in surface area of Al-MCM-41 after incorporation of Fe-TPyP. This decrease could be due to a partial blocking of pores of MCM-41 by Fe-TPyP.

The existence of Fe-TPyP in Fe-TPyP-Al-MCM-41 and Fe-TPyP-PMAA were also supported by chemical and thermal analysis (see entries 4 and 5 in Table 1). It shows that the molar amount of Fe and porphyrin is almost equal, suggesting that the catalysts contain no free Fe or TPyP.

3.2. Long-range order structure of iron-porphyrin encapsulated in Al-MCM-41

X-ray powder diffraction patterns of mesophase Al-MCM-41, calcined Al-MCM-41 and Fe-TPyP-Al-MCM-41 (Fig. 5), which are in excellent agreement with the XRD pattern for unloaded molecular sieve without any peaks arisen

Table 1
Catalytic oxidation of benzene to phenol^a

Entry	Catalyst	Fe (μmol)	Porphyrin (μmol)	Surface area of catalyst ($\text{m}^2 \text{g}^{-1}$)	Phenol yield (μmol)	TON per Fe
1	None	–	–	–	0.0	–
2	Fe-TPyP	–	–	–	0.0	–
3	Al-MCM-41	–	–	1064	2.0	–
4	Fe-TPyP-PMAA	0.030 ^b	n.a. ^c	48	30.0	1000
5	Fe-TPyP-Al-MCM-41	0.150 ^b	0.14 ^d	497	10.0	67
6	Fe-TPyP-Al-MCM-41 reused ^e	0.150 ^b	–	–	10.0	–
7	Fe-TPyP-PMAA reused ^e	0.025 ^b	–	–	25.0	–

^a All reactions were carried out at 70 °C for 20 h with benzene (2 ml), 30% H₂O₂ (1 ml) and catalyst (50 mg) with vigorous stirring.

^b The concentration of Fe was measured absorption spectrometer.

^c Not available. We failed to determine the amount of TPyP in its mixture with PMAA.

^d The concentration of porphyrin was analyzed by Thermal Gravimetry Analyzer.

^e The reaction was performed after washing and drying of the catalyst.

from Fe-TPyP. A typical XRD pattern after encapsulation of the Fe-TPyP complex showed weak peaks of (1 1 0), (2 0 0) and (2 1 0) in the 2θ range 3.5–6.0 indicating that the long range order of the inorganic host, Al-MCM-41 has decreased after the encapsulation, but fundamentally the mesostructure of the host materials is still maintained. This suggests that that ordered Al-MCM-41 could still be obtained during the encapsulation of Fe-TPyP complexes. The Fe-TPyP lines are not observed in XRD of the encapsulated material because the amount of Fe-TPyP is considerably small. As shown in Table 1, it is also revealed that the surface area of Fe-TPyP-Al-MCM-41 is much smaller compared to those of

Al-MCM-41. These observations provide strong support for the suggestion that incorporation of Fe-TPyP complexes, presumably in internal pore, occurs in Fe-TPyP-Al-MCM-41.

3.3. Catalytic properties for oxidation of benzene

Table 1 shows the activities of iron-porphyrins for direct oxidation of benzene to phenol using aqueous H₂O₂ in solution and supported on molecular sieve and polymer. Unexpectedly, reaction system containing Fe-TPyP catalyst is not active in the oxidation reaction. Fe-TPyP-Al-MCM-41 and Fe-TPyP-PMAA give raise higher activity than Fe-TPyP (entries 4 and 5 in Table 1). This is supported by the rate of the formation of phenol over Fe-TPyP-Al-MCM-41 and Fe-TPyP-PMAA (see Fig. 6). The most likely reason for the high activity of Fe-TPyP encapsulated in Al-MCM-41 and PMAA is the presence of Fe-TPyP coordination to molecular sieve or polymer, which render them more resistant to oxidative self-destruction.

The turnover number (TON), the molar ratio of the phenol to the loaded Fe for the reaction with Fe-TPyP-PMAA was almost 15 times higher than that of Fe-TPyP-Al-MCM-41

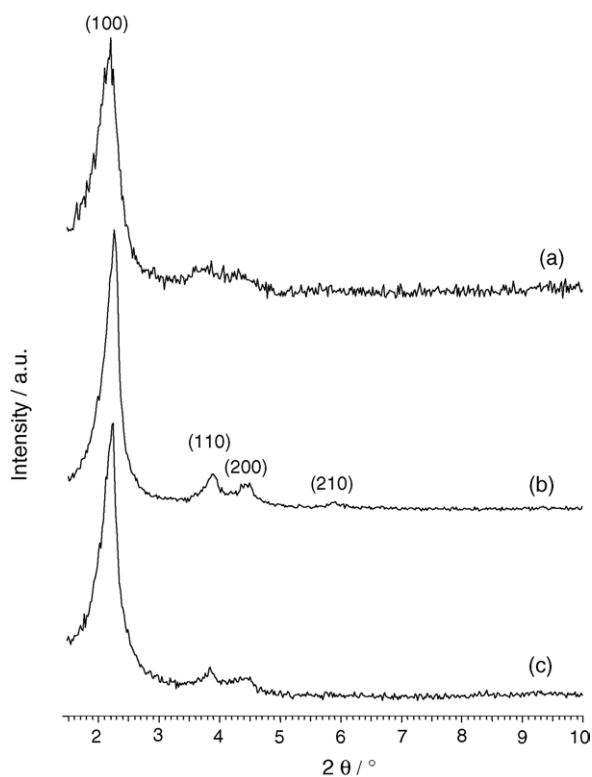


Fig. 5. X-ray diffractograms of (a) as-synthesized Al-MCM-41, (b) calcined Al-MCM-41 and (c) Fe-TPyP-Al-MCM-41.

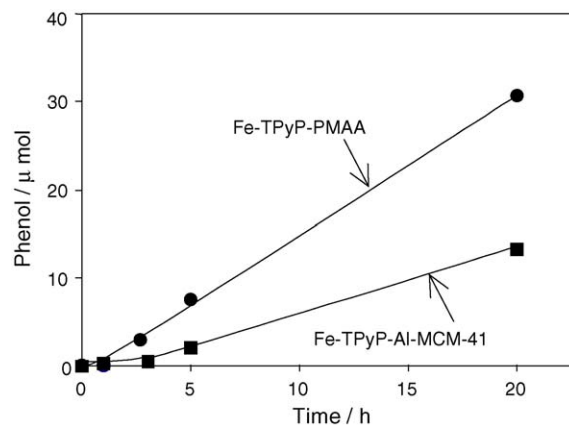


Fig. 6. The oxidation rate of benzene to phenol using Fe-TPyP-PMAA and Fe-TPyP-Al-MCM-41 catalysts. All reactions were carried out at 70 °C with benzene (2 ml), 30% H₂O₂ (1 ml) and catalyst (50 mg) with vigorous stirring.

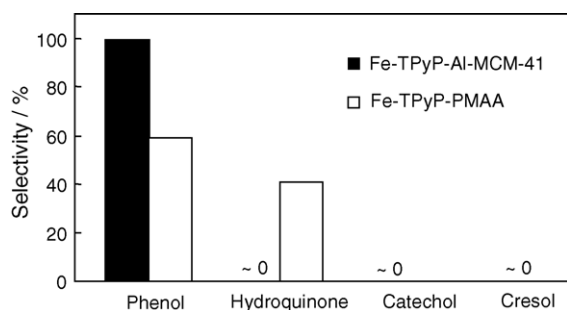


Fig. 7. The product selectivity of oxidation of benzene with aqueous hydrogen peroxide using Fe-TPyP-PMAA and Fe-TPyP-Al-MCM-41. All experiments were done similar to that of reaction conditions shown in Fig. 2.

(entries 4 and 5 in Table 1). If the surface area of catalysts is taking into consideration, the TON per surface area for the reaction with Fe-TPyP-PMAA becomes much more higher compared to that of Fe-TPyP-Al-MCM-41. It confirms that the oxidation of benzene to phenol is efficiently catalyzed by Fe-TPyP-PMAA.

The recovered and dried Fe-TPyP-Al-MCM-41 and Fe-TPyP-PMAA catalysts were reused in a fresh reactant mixture and showed 100% and ca. 75% activities, respectively (entries 6 and 7 in Table 1). The decrease in activity of recovered Fe-TPyP-PMAA may be attributed to leaching of the active sites (entry 7 in Table 1). A negligible decrease in activity of recovered Fe-TPyP-Al-MCM-41 is observed because there is no leaching of Fe-TPyP occurs during the reaction (entry 6 in Table 1). A strong electrostatic interaction of Fe-TPyP and Al-MCM-41 might play a role to prevent the leaching of the Fe-TPyP species. In summary, although Fe-TPyP-PMAA showed higher activity compared to Fe-TPyP-Al-MCM-41, the regenerability of Fe-TPyP-PMAA is not as good as that of Fe-TPyP-Al-MCM-41.

Fig. 7 shows the product selectivity of Fe-TPyP-Al-MCM-41 and Fe-TPyP-PMAA catalysts toward oxidation of benzene. GC analyses indicated that phenol was the sole product in the oxidation of benzene over Fe-TPyP-Al-MCM-41 and other probable by-products such as hydroquinone, catechol or cresol, were not produced. The product selectivity of Fe-TPyP-PMAA toward the production of phenol was 60%, since 40% hydroquinone was also produced.

Based on the above discussions, one considers that the hydrophobic nature of Fe-TPyP-PMAA may account for the high catalytic activity, and the ordered structure of Fe-TPyP-MCM-41 may contribute to a high selectivity in oxidation of benzene with aqueous hydrogen peroxide.

4. Conclusions

Fe-TPyP complexes were successfully prepared by incorporating Fe-TPyP within mesoporous molecular sieve Al-MCM-41 (Fe-TPyP-Al-MCM-41) and poly(methacrylic acid) (Fe-TPyP-PMAA) as inorganic and organic supports, respectively. The Fe-TPyP-PMAA showed higher activity

compared to Fe-TPyP-Al-MCM-41. However, the regenerability of Fe-TPyP-PMAA is not as good as that of Fe-TPyP-Al-MCM-41. One considers that the hydrophobic nature of Fe-TPyP-PMAA may account for the high activity, and the ordered structure of Fe-TPyP-MCM-41 may contribute to a high selectivity.

Acknowledgement

The authors gratefully acknowledge the Ministry of Science, Technology and Environment (MOSTE) for the financial support under IRPA grant 09-02-06-0057-SR0005/09-04.

References

- [1] J.R. Lindsay-Smith, R.A. Sheldon (Eds.), *Metalloporphyrin in Catalytic Oxidations*, Marcel Dekker, New York, 1994.
- [2] Y. Iamamoto, K.J. Ciuffi, H.C. Sacco, L.S. Iwamoto, O.R. Nascimento, C.M.C. Prado, *J. Mol. Catal. A* 116 (1997) 405.
- [3] C.M.C.P. Manso, E.A. Vidoto, F.S. Vinhado, H.C. Sacco, K.J. Ciuffi, P.R. Martins, A.G. Ferreira, J.R.L. Smith, O.R. Nascimento, Y. Iamamoto, *J. Mol. Catal. A* 150 (1999) 251.
- [4] S.L.H. Rebelo, M.M.Q. Simoes, M.G.P.M.S. Neves, J.A.S. Cavaleiro, *J. Mol. Catal. A* 201 (2003) 9.
- [5] C. Paul-Roth, F.D. Montigne, G. Rethore, G. Simonneaux, M. Gulea, S. Masson, *J. Mol. Catal. A* 201 (2003) 79.
- [6] Y. Terazono, D. Dolphin, *Inorg. Chim. Acta* 346 (2003) 261.
- [7] J.Y. Liu, X.F. Li, Z.X. Guo, Y.Z. Li, *J. Mol. Catal. A* 179 (2002) 27.
- [8] M.A. Schiavon, Y. Iamamoto, O.R. Nascimento, M.D. Assis, *J. Mol. Catal. A* 174 (2001) 213.
- [9] Z. Li, C.G. Xia, X.M. Zhang, *J. Mol. Catal. A* 185 (2002) 47.
- [10] C.T. Kresge, M.E. Leonowicz, W.J. Roth, J.C. Vartuli, J.S. Beck, *Nature* 359 (1992) 710.
- [11] J.S. Beck, J.C. Vartuli, W.J. Roth, M.E. Leonowicz, C.T. Kresge, K.D. Schmitt, C.T.-W. Chu, D.H. Olson, E.W. Sheppard, S.B. McCullen, J.B. Higgins, J.L. Schlenker, *J. Am. Chem. Soc.* 114 (1992) 10834.
- [12] Q. Huo, D.I. Margolese, U. Ciesla, P. Feng, T.E. Gier, P. Sieger, R. Leon, P.M. Petroff, F. Schüth, G.D. Stucky, *Nature* 368 (1994) 317.
- [13] P.T. Tanev, T.J. Pinnavaia, *Science* 267 (1995) 865.
- [14] A. Corma, *Chem. Rev.* 97 (1997) 2373, and references therein.
- [15] E.M. Serwicka, J. Poltowicz, K. Bahranowski, Z. Olejniczak, W. Jones, *App. Catal. A* 275 (2004) 9.
- [16] M.R. Kishan, V.R. Rani, M.R.V.S. Murty, P.S. Devi, S.J. Kulkarni, K.V. Raghavan, *J. Mol. Catal. A* 223 (2004) 263.
- [17] J. Poltowicz, E.M. Serwicka, E. Bastardo-Gonzalez, W. Jones, R. Mokaya, *Appl. Catal. A* 218 (2001) 211.
- [18] C.-J. Liu, S.-G. Li, W.-Q. Pang, C.-M. Che, *Chem. Commun.* (1997) 65.
- [19] K. Weissmermel, H.-J. Arpe, C.R. Lindley, S. Hawkins, *Industrial Organic Chemistry*, fourth ed., Wiley-VCH, Weinheim, 2003.
- [20] Z. Luan, C.F. Cheng, W. Zhou, J. Klinowski, *J. Phys. Chem.* 99 (1995) 1018.
- [21] I.L.V. Rosa, C.M.C.P. Manso, O.A. Serra, Y. Iamamoto, *J. Mol. Catal. A* 160 (2000) 199.
- [22] S. Nakagaki, A.R. Ramos, F.L. Benedito, P.G. Peralta-Zamora, A.J.G. Zarbin, *J. Mol. Catal. A* 185 (2002) 203.
- [23] A.C. Voegtlin, A. Matijasic, J. Patarin, C. Sauerland, Y. Grillet, L. Huve, *Microporous Mater.* 10 (1997) 137.